

REVIEW

PACS numbers: 42.55.Rz; 42.55.Xi; 42.60. – v
DOI: 10.1070/QE2009v039n01ABEH013787

Diode-side-pumped laser heads for solid-state lasers

S.G. Grechin, P.P. Nikolaev

Contents

***Abstract*. Principal configurations of diode-side-pumped laser heads for solid-state lasers are considered. A comparative analysis is performed for radiation characteristics of lasers with such laser heads.**

Keywords: *solid-state lasers, diode pumping, laser head, laser radiation parameters.*

1. Introduction

Diode-pumped solid-state lasers (SSLs) are actively used for solving various problems in science and technology. Such lasers constituted about 30 % in the total sales volume of SSLs in 2006 [1] and this part is still growing. Compared to flashlamp-pumped SSLs, they exhibit a number of important advantages including the efficiency that is an order of magnitude greater because laser diodes have a high efficiency of converting electric power into the power of optical radiation which achieves 60 %. In addition, these diodes possess a comparatively narrow (2 – 5 nm) emission line, which can be matched with an absorption spectrum of activator ions. Output parameters of laser radiation can be easily stabilised due to a short response time of laser diodes. Diode-pumped SSLs are reliable and have a long lifetime. This life for modern pump diodes exceeds 10000 hours and there are diodes with the lifetime of 1 million hours. The absence of UV components in the emission spectra of pump diodes ensures a longer service life for active elements because the radiation-induced colouration of crystals and formation of colour centres are excluded as well as the chemical decomposition of cooling agent in the laser head cooling system. The use of diode pumping provides much higher power of output radiation due to a higher density of the pump power. Diode-pumped SSLs are small in size, their cooling, electrical, and control systems consume leass power and are more compact. Nevertheless, with all these advantages they have a serious drawback, namely, high cost, which is determined by expensive pump diodes (about \$10 – \$20 per watt). However, each year their cost falls and according to the forecasts will tend to \$1 per watt. This drawback, in turn, is compensated by low maintenance charges.

In recent years diode-pumped SSLs are intensively developed and investigated. It is important to analyse the modern state-of-the-art of these studies and define the tendencies of their evolution. Basic directions in developing diode-pumped SSLs were considered in [2]. Improving the construction of laser heads is a key problem in developing such SSLs aimed at obtaining the maximum efficiency of the pump radiation absorption in an active element and providing a required distribution profile of the inverse population cross section. General principles for constructing flashlamp-pumped and diode-pumped laser heads were described in [3]. Various applications of SSLs place quite contradictory requirements to the output characteristics of such lasers. Various pump schemes for SSLs are used in order to meet these requirements. Presently, numerous realisations of the pump schemes are suggested. They have certain advantages and drawbacks (limitations), which determine their possible applications. In this work we

S.G. Grechin, P.P. Nikolaev Scientific Research Institute for Radioelectronics and Laser Technology, N.E. Bauman Moscow State Technical University, 2-ya Baumanskaya ul. 5, 107005 Moscow, Russia; e-mail: gera@bmstu.ru

Received 26 December 2007; revision received 5 May 2008
Kvantovaya Elektronika **39** (1) 1 – 17 (2009)
Translated by N.A. Raspopov

present some principal variants of side diode pumping for SSL by using data available in literature. A particular attention is paid to laser heads for lasers with the average power of up to tens or hundreds of watts, which are most often used in practice.

In most papers considering new laser head schemes, the generation parameters are mainly analysed for the lasers based on such laser heads and, as a rule, no results of investigations on laser heads themselves are presented. Therefore, in this work laser heads are characterised by the corresponding parameters of laser radiation. Note also that many papers are devoted to laser heads operating in a cw or quasi-cw regimes widely used in practice. Works devoted to laser heads for pulsed lasers are few and are not considered here.

2. Schemes for pumping active elements

There are two principal methods for diode pumping an active medium, namely, end and side pumping. The former one concerns with the schemes in which pump radiation is coupled into an active element of the SSL along its optical axis (the propagation direction for the laser radiation) or is slightly inclined to it. Such a pump scheme provides a high efficiency and single-mode generation in addition to well stabilised output parameters. This is explained by the good spatial matching of the pumped volume of the active element with the generated mode volume, small cavity length, and a small number of elements to be adjusted. But the end scheme does not allow a large volume of active element to be pumped. Special optics and elements are used for coupling radiation, which increases the cost of the pump system and reduces its efficiency. In addition, the end of the active element through which it is pumped is subjected to great radiation and thermal loads. Taking the above into account, end-pumped SSLs are more preferable as master oscillators and sources of radiation with average powers of several or tens of watts.

Since the origin of semiconductor pump sources the schemes with side pumping are most often used in SSL constructions especially at moderate and high powers. In schemes with side pumping, radiation is coupled into the active element through the lateral surface, which allows pumping the whole volume of the active medium without complicated schemes of radiation input. This provides simple and efficient scaling of the SSL output power and uniform absorption of pump radiation over the active element volume thus reducing a thermal load on the latter. In this paper, we consider the laser heads with side pumping most completely presented in publications.

3. Schemes with side pumping

Note that the construction of a side-pumped laser head is mainly determined by the approach in designing the scheme for pumping an active element. There are two approaches: pumping with a small number of passes and multipass pumping, which is determined by the number of passes of pump radiation through the cross section of a cylindrical active element. In most cases we deal with a small number of passes and the most of pump radiation is mainly absorbed during the first passage through the active element. By choosing the geometrical dimensions of laser heads, activator concentration in the active element, and pump radiation parameters one can provide formation of the required distribution of inverse population across the element cross section. In some papers, multipass pumping is used with a small absorption of radiation per passage. This enhances the uniformity of the inverse population distribution over the cross section, however, the quality requirements to the used materials and elements are stronger.

Regardless of the approach to a pump scheme, the following elements and units are used in a laser head construction: an active element, pump source, unit for coupling radiation, and reflector. The optimal parameters of these elements are closely interelated and require a complex approach to their consideration. In designing a laser head, the starting points are an active element and diode pump source. Choosing the active element, one should solve the traditional problems concerning its material and shape, activator concentration, delustering of a lateral surface, cooling system. Spectroscopic, thermal and mechanical properties of active media most widely used are presented in [4]. The choice of a diode pump source is reduced to the arrangement of semiconductor structures. Most of papers are devoted to investigations of laser heads for lasers operating in a cw or quasi-cw regimes. In these regimes, diode bars are widely used. Diode arrays capable of producing radiation with a higher power density are rarely used. However, their advantage cannot be realised due to a high specific power of released heat, inhomogeneous heating of elements in the array, and, consequently, increased width of the emission spectrum. The way of coupling pump radiation into an active element is also important, as well as characteristics of the reflector in a laser head. These two parameters directly affect the laser head performance. One of the parameters characterising a laser head as a whole is the efficiency of the pump radiation absorption. In developing a laser head, the problem of obtaining the maximum efficiency is usually posed. One more important laser head parameter is the inverse population distribution over the cross section of the active element, which is determined by the scheme of pump radiation coupling, the generatrix of the active element, and geometrical parameters of the laser head itself.

In most works, optimisation of a laser head is aimed at forming a homogeneous distribution of the pump power over the cross section. Thus, we can, on the one hand, completely use the volume of the active element, and on the other hand, realise the parabolic temperature distribution over the active element cross section, which makes it possible to efficiently compensate for thermooptical distortions by traditional methods of linear optics. The reverse side is the decrease in the total SSL efficiency especially during single-mode operation due to concentration of generating modes mainly around the axis of the active element.

4. Pumping of cylindrical elements

In such constructions a cylindrical element is placed in a glass tube with a cooling agent. Diode pump sources are placed along the generatrix of the tube (reflector). Around the tube with the active element there is a diffuse or mirror reflector with windows for coupling pump radiation into the active element. The pump radiation is introduced either by using an auxiliary optical system (cylindrical lenses,

optical fibres, thin plates, lens ducts, etc.) or without it (direct pumping). The advantages of a conventional scheme are relative simplicity, low cost and compactness of the design, and good scalability with respect to power. This scheme provides high power densities per length of the active element.

However, this scheme has drawbacks as well. Among all possible shapes, a circle has the shortest length at a prescribed cross-section area. This prevents efficient cooling of the entire volume of the active element, thermal effects being more pronounced in a cylindrical active element. Consider in more detail the experimentally tested schemes with side pumping.

4.1 Schemes with direct pumping

A scheme with a cylindrical diffuse reflector and direct input of radiation [5–16] (see Fig. 1) is simple, compact, though efficient for side pumping of a cylindrical element. The reflector is assembled from several segments of a diffusely scattering material (the number of segments depends on the number of input windows) and has the 10–15-mm diameter of the inner reflecting surface. Pump radiation is coupled into the reflector through narrow input windows (the width is usually 0.5–2 mm) with no auxiliary optics. The input windows are air gaps between the elements of the diffuse reflector. Emitting assemblies of pump diodes are placed close to the input windows. Usually there are three (rarely five) assemblies. The thickness of the diffuse reflector near the input windows is less than 1 mm. The absence of auxiliary optics eliminates losses spent on additional reflection and absorption. Inside the reflector there is a cylindrical active element with a glass tube of the cooling system on which an antireflection coating at the pump radiation wavelength is deposited. In such a laser head, almost uniform distribution of luminescence was obtained [7] (see Fig. 2).

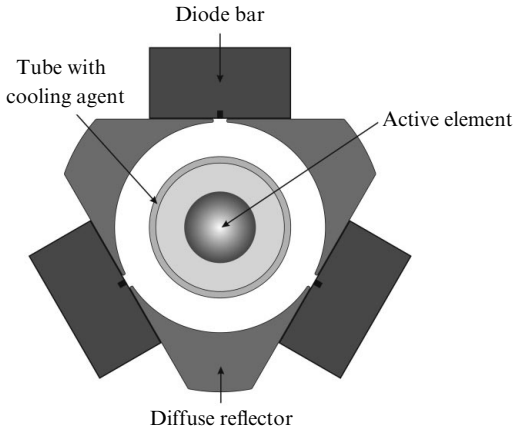

Figure 1. Scheme of a laser head with a diffuse reflector [5–16].

In some cases, a diffuse reflecting coating is directly deposited onto the external generatrix of the cooling system tube [9, 17]. The diffuse reflector along with a small activator concentration in the active element makes it possible to achieve a highly uniform profile of absorbed pump radiation due to a greater number of pump radiation transits across the active element. When a high-quality diffuse reflector (with the reflection coefficient of up to

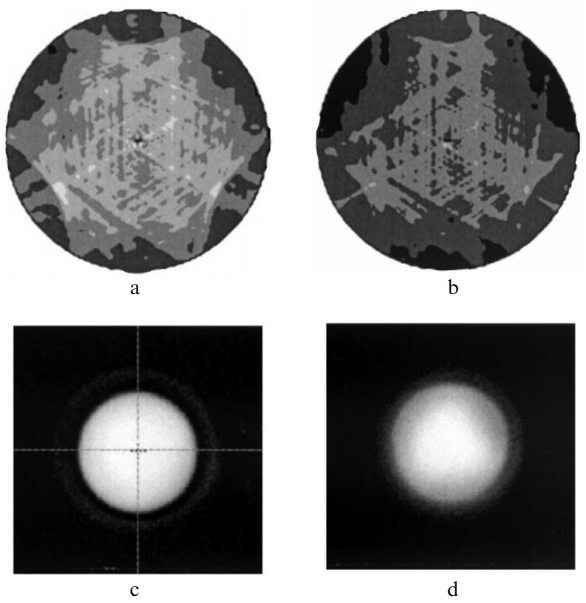

Figure 2. Calculated distributions of the absorbed energy (a, b) and the corresponding measured distributions of luminescence (c, d) across the cross section of the active element with the diameter of 5 mm (a, b) and 6 mm (c, d) [7].

99 %) is used, the efficiency of the pump radiation absorption can reach 90 % [5, 11]. Thus, for Nd^{3+} : YAG lasers the slope efficiency of $\eta_{sl} \leqslant 65\,65\%$ is achieved [8] and the total efficiency is $\eta_{opt} \leqslant 49\,\%$ [16] (see Table 1).

The main problem in realising the scheme under study is exact matching of the transmitting aperture of pump diodes with the input windows [5]. In addition, at high pump powers a diffuse reflector requires cooling because of the compactness of pump sources and the presence of absorption in a diffusely scattering material.

In [7], the influence of the active element diameter, reflector diameter, and activator concentration on the efficiency of the pump radiation absorption and on the profile of the pump power distribution across the active element was investigated theoretically and experimentally. An optimal combination of these parameters was also suggested. The absorption efficiency decreases with increasing the reflector diameter; however, the inverse population distribution over the active element cross section becomes more uniform. Based on these facts authors in [7] chose the reflector with a diameter of 16 mm for an active element 5 mm in diameter. These parameters determined the optimal concentration of the activator (0.6 %).

In [9], the influence of the size (width) of input windows on the efficiency of the pump radiation absorption in the active element was thoroughly studied. It was shown that there exists an optimal window width. At a small width, not all pump radiation is coupled into the reflector, and at a larger width, a noticeable part of radiation unabsorbed in the active element escapes the reflector. In the geometry considered in [9] the optimal window width is 2 mm. Widths of windows used in other papers are presented in Tables 1 and 2.

Note that Nd^{3+} : YAG active elements with a low activator concentration can be grown by the horizontal directed crystallisation technique, which differs from Czochralski technique. In this case, a high optical quality is obtained.

Table 1. Radiation parameters for laser laser heads with a diffuse reflector.

d_{ae}/mm	C_a (%)	D_r/mm	s_w/mm	N_p	Delustering	η_{sl} (%)	η_{opt} (%)	P_p/W	P_{out}/W	Generation regime	$\frac{P}{L_p}$/W cm^{-1}	M^2	F_{th} (D)	References
4	0.8	12	0.7	3	+	53.4	34.3	182.0	62.4	cw	49.2	45	2.9	[5]
3	0.6	13	1.2	3	+	49.0	29.4	335.0	98.3	cw	47.9	10	5.7	[6]
5	0.6	16	1.3	3	+	49.0	46.7	1070.0	500.0	cw	152.9	–	–	[7]
5	0.6	–	–	3	+	64.7	45.0	1720.0	776.0	cw	–	72	7.1	[8]
3	1.0	10	2.0	3	–	35.2	22.0	400.0	88.0	cw	–	–	–	[9]
4	0.6	12	1.5	3	+	42.1	34.5	400.0	138.0	cw	44.4	75	4.8	[11]
3.5	0.6	12	–	3	–	–	23.1	476.0	110.0	cw	103.5	17	2.5	[12]
7	0.7	–	–	5	–	–	35.9	150.0	53.8	qcw	–	40	4.5	[13]
3	0.6	–	–	3	–	–	16.5	135.0	22.3	qcw	–	1.3	–	[14]
3.5	0.6	12	1.3	3	+	55.1	48.8	434.0	211.6	cw	96.4	19	4.5	[16]

Notes: active element is Nd^{3+}:YAG (1064 nm); d_{ae} is the active element diameter; C_a is the activator concentration; D_r is the reflector diameter; s_w is the slit width for coupling pump radiation; N_p is the number of pump sources; P_p is the pump radiation power; P_{out} is the output power of laser radiation; P/L_p is the linear density of the pump radiation power; L_p is the length of the pumped region; M^2 is the parameter of the laser beam quality; F_{th} is the thermal lens power for the active element; cw and qcw refer to cw and quasi-cw laser operation regimes.

Table 2. Radiation parameters for laser laser heads with a mirror reflector.

d_{ae}/mm	C_a (%)	D_r/mm	s_w/mm	N_p	η_{sl} (%)	η_{opt} (%)	P_p/W	P_{out}/W	$\frac{P}{L_p}$/W cm^{-1}	M^2	F_{th} (D)	References
4	0.8	12	1.5	3	35.3	26.0	400.0	104.0	44.4	–	4.8	[11]
2	1.0	–	–	3	21.8	17.0	100.0	17.0	–	–	–	[17]
3	1.0	–	–	3	29.5	24.5	100.0	24.5	–	–	–	[17]
4	1.0	–	–	5	21.0	18.5	542.0	100.0	–	73 × 82	9.1	[18]
6	0.8	12	–	4	36.9	33.3	2400.0	800.0	150.0	74	10.0	[19]
4	0.8	–	1.0	3	44.6	37.5	400.0	150.0	100.0	24	7.7	[20]
4	0.9	10	1.5	3	54.3	46.1	423.0	195.0	–	58	–	[21]
4	0.6	10	1.5	3	12.6	11.7	262.0	30.5	117.5	20	7.0	[22]
4	0.9	–	–	3	46.0	23.6	555.0	131.0	111.0	51	7.7	[23]
4	0.9	–	–	3	40.0	21.8	555.0	121.0	–	34 × 43	–	[24]

Notes: active element is Nd^{3+}:YAG (1341 nm) [18, 24], Nd^{3+}:YAG (second harmonic, 532 nm) [22], Nd^{3+}:YAG (1319 and 1338 nm) [23], and Nd^{3+}:YAG (1064 nm) in the rest references; all the lasers operated in a cw regime; in the case of homocentric beams, the product $M_x^2 \times M_y^2$ is used instead of M^2; notations are the same as those in Table 1.

The use of a mirror reflector instead of a diffuse one provides a higher efficiency of the pump radiation absorption due to its higher reflection coefficient [17–24]. Nevertheless, a mirror reflector noticeably deteriorates the uniformity of the absorbed pump power profile due to strong focusing of pump radiation (mirror reflectors are mainly cylindrical in shape). A comparative analysis of pump schemes with diffuse and mirror reflectors is presented in [11, 17]. Figure 3 shows the generation characteristics for a Nd^{3+}:YAG laser (the concentration of neodymium is 1 %) with various types of reflectors and various diameters of the active element [17]. The slope efficiency of SSLs with a mirror reflector is lower by 5 %–10 %, which is mainly related to worse uniformity of the absorbed pump power profile.

To make absorption of pump radiation more uniform, the beam in the active element should be collimated. For this purpose, the output aperture of pump diodes should be placed in the front focus of the optical system formed by the adjoining surfaces of tube, cooling agent, and active element [11]. In the case of a mirror reflector and direct pumping of the active element, the efficiency of the pump power absorption is 94 % [21]. Thus, for Nd^{3+}:YAG lasers the slope efficiency is $\eta_{sl} \leqslant 54$ % and total efficiency is $\eta_{opt} \leqslant 46$ % [21] (see Table 2). Gold [11, 19, 21, 25], silver [20], and copper [22] are traditionally used for HR coatings. Copper exhibits the best adhesion among them, and silver coatings possess the largest reflection coefficient.

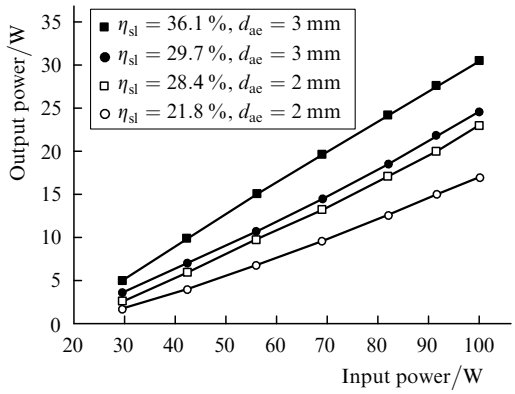

Figure 3. Generation characteristics of a Nd^{3+}:YAG laser with diffuse (squares) and mirror (circles) reflectors [17].

Mirror reflecting coatings can be deposited either on the inner surface of a cylindrical reflector [19] (see Fig. 4a) or on the outer surface of the cooling system tube (see Fig. 4b). In the first case, the reflector comprises several parts with narrow air gaps between them used for coupling pump radiation into the reflector cavity. In the second case, narrow slits are made on the reflecting coating, through which pump radiation passes. The output windows are necessarily AR coated at the pump radiation wavelength.

In some papers [21, 22] it is shown that input windows may not have AR coatings. If an emitting diode is inclined

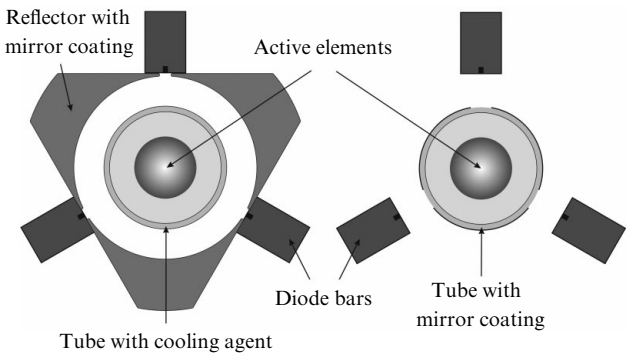

Figure 4. Various realisations of laser heads with mirror reflectors [17 – 24].

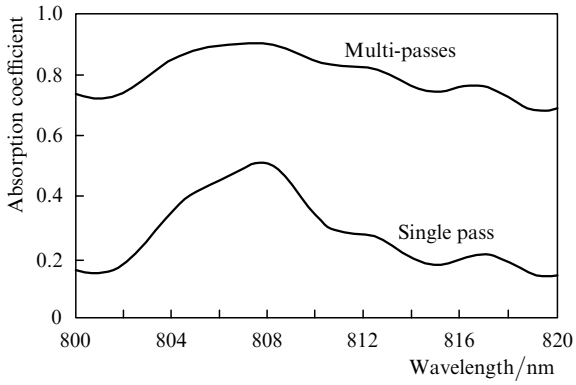

Figure 6. Absorption efficiency as a function of the wavelength [26].

at the Brewster angle to the normal of the cylindrical surface of the tube, the losses due to the reflection from a media interface are small. The polarisation of pump radiation should be directed along the optical axis of the tube (π-polarisation).

At relatively low pump powers, the mirror coating can be deposited directly onto the cylindrical generatrix of an active element [26 – 28] (see Fig. 5). Similarly to the previous case (with the tube), the reflecting coating has narrow windows with AR coatings at the pump radiation wavelength. This scheme provides a high efficiency of the pump power absorption (above 90 %) at a small diameter of the active element (less than 2 mm) [26]. Obvious advantages of this scheme are simplicity and air cooling of the active element (usually the latter is placed into a copper heatsink) [28]. The closed cooling system reduces the accuracy of adjusting the wavelength (or temperature of elements) of the pump sources. Figure 6 presents the wavelength dependence of the absorption efficiency per single pass and per several passes through the active element without an AR coating [26].

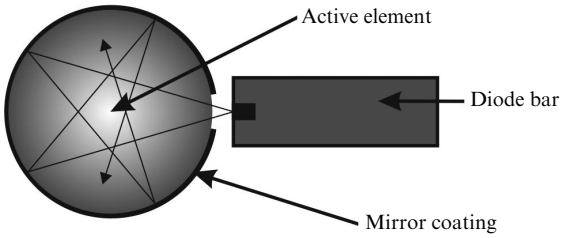

Figure 5. Pump scheme [26 – 28].

As was mentioned above, the main drawback of a cylindrical mirror reflector is the strong focusing of pump radiation, which negatively affects the homogeneity of the absorbed pump power profile. To avoid this, designers use reflector shapes instead of the traditional cylindrical one. In some papers it was proposed to use cylindrical surfaces of a larger radius [17] (see Fig. 7a) or plane surfaces [25] (see Fig. 7b) as reflecting elements. In [29], the pump scheme was proposed with a cusp-shaped reflector similar to that used in solar-pumped lasers (see Fig. 7c). Various pump schemes comprising prism reflectors with a triangle cross section were thoroughly investigated in [30 – 33] from the viewpoint of forming the pump power distribution, thermal fields, and thermoelastic stresses in the active element.

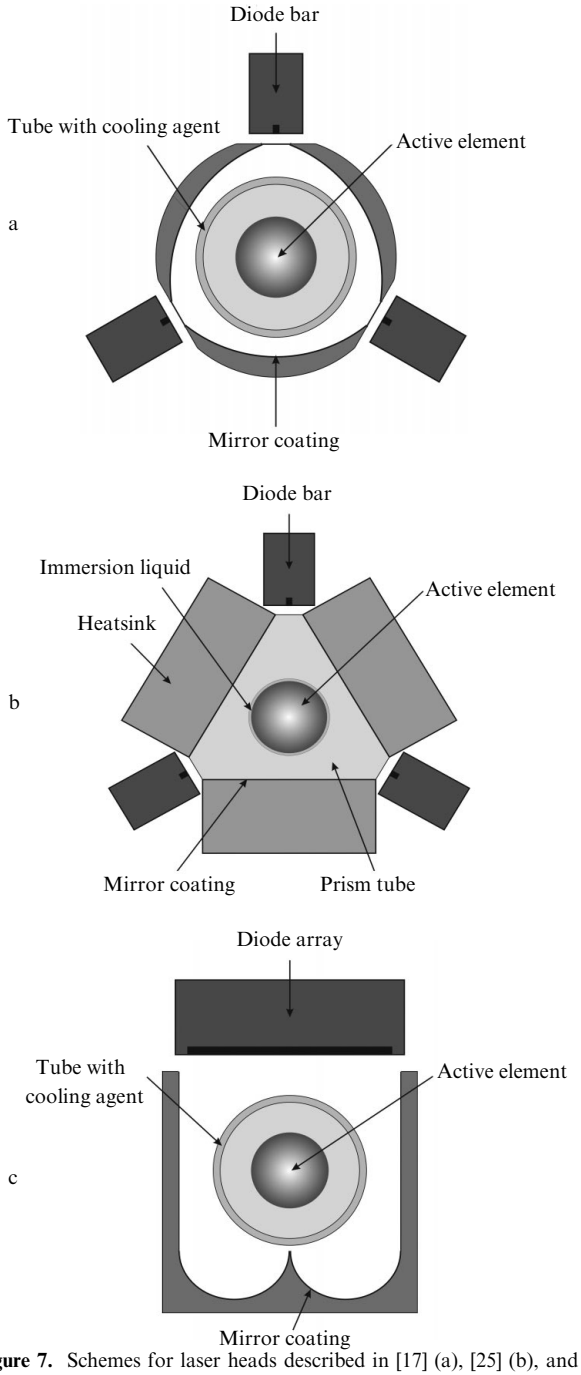

Figure 7. Schemes for laser heads described in [17] (a), [25] (b), and [29] (c).

The scheme [25] presented in Fig 7b deserves a particular attention. It realises the idea of side pumping of a cylindrical active element with 'dry' conductive cooling. A triangular prism reflector made of MgF_2 possessing high thermal conduction is also a part of a heatsink system. The active element has an optical and thermal contact with the prism reflector due to a thin (the width is ~ 100 μm) liquid layer between them. By using this scheme for pumping a Nd^{3+} : YLF active element the output power of 72 W was obtained in the multimode regime at the slope efficiency $\eta_{sl} = 49\,\%$ and beam quality parameter $M^2 = 8$. This construction of the laser head is specific in that the thermooptical distortions induced in the active element differ by a factor of almost two for the total and central (75 % by the cross section area) apertures of the active element in the entire range of pump powers. This difference is typical of laser heads with a small number of pump sources at a small number of radiation passes through the active element.

A side pumping scheme without an external reflector is most simple from the viewpoint of the construction though the least efficient [34 – 37]. In the absence of the reflector pump radiation should be absorbed in the active element per single pass. Hence, the activator concentration should be sufficiently high, which deteriorates the optical quality and spectroscopic parameters of the active element. This scheme cannot be used for pumping active elements with a small diameter due to a weak absorption per single pass. A uniform profile of the absorbed pump power can be obtained at a large number (more than five) of emitting diode bars surrounding the active element. Such a scheme is characterised by a low efficiency of the pump power absorption.

4.2 Schemes with optical systems for coupling pump radiation

The main drawback of direct pumping is a low pack density of laser diode bars around the active element because of the large transverse dimensions of pump sources. For obtaining a high efficiency of the pump power absorption, the diameter of a diffuse reflector should not be greater than 10 – 15 mm [7]. In such a geometry, no more than three – five bars can be arranged closely to the reflector around the active element. This prevents obtaining a high pump power density per unit length of the active element. The use of a greater number of bars requires mounting them at a longer distance from the active element, which necessitates the employment of an optical focusing system for coupling radiation and matching the dimensions of the pumped region with the output aperture. Because any optical system introduces losses, its employment reduces the efficiency of the pump power absorption and noticeably complicates the construction of a laser head, its mounting and adjustment. In addition, optical systems for radiation coupling considerably increase the cost of the laser head.

A variant of coupling pump radiation is the use of thin glass plates [38 – 44] (see Fig. 8). A diode bar is placed in the vicinity of one end of the plate, whereas the other end is put into the cavity of a diffuse reflector. The surfaces of both ends have an AR coating at the pump radiation wavelength. Pump radiation propagates along the plate due to the total internal reflection from its lateral surfaces. The coefficient of the pump radiation transfer through such plates achieves 97 % – 98 % [38 – 41]. The total efficiency of the pump power absorption is 89 % [39]. Thus, for a Nd^{3+} : YAG laser we have $\eta_{sl} \leqslant 53\,\%$ [39] and $\eta_{opt} \leqslant 38\%$ [38] (see Table 3).

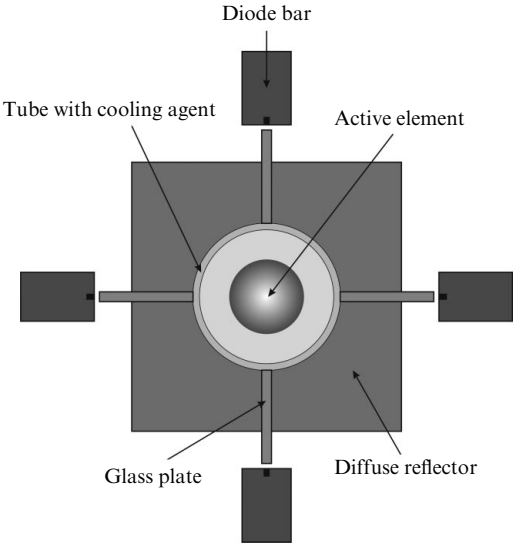

Figure 8. Scheme of a laser head with glass plates used for coupling pump radiation [38 – 44].

The use of diode arrays instead of diode bars or a transverse disposition of the bars relative to the axis of active element can give even greater densities of the pump power. In these cases, special lens ducts (wedge lens, lens duct, etc.) are used for coupling pump radiation into the active element. The pump beam, propagating in these elements due to the total internal reflection, is compressed by several times (usually by a factor of 8 – 10) in the direction normal to the optical axis of the active element. The beam divergence increases by the same factor, which provides a more uniform pumping of the active element.

In [45, 46], a scheme of the laser head is presented with

Table 3. Radiation parameters for laser laser heads with glass plates used for coupling pump radiation.

d_{ae}/mm	C_a (%)	N_p	η_{sl} (%)	η_{opt} (%)	P_p/W	P_{out}/W	Generation regime	M^2	F_{th} (D)	References
4	–	4	41.3	37.8	352.0	133.0	cw	46	–	[38]
4	0.8	2	52.2	29.6	135.1	40.0	cw	80	–	[39]
4	0.6	2	34.3	27.7	140.8	39.0	cw	40	–	[40]
4	0.6	4	33.3	27.8	352.0	98.0	cw	45	3.9	[41]
4	0.6	4	38.4	36.0	322.0	116.0	cw	–	3.1	[42]
4	0.6	4	34.2	25.6	800.0	205.0	cw	11	–	[43]
4	0.6	4	45.8	37.2	296.0	110.0	qcw	17	–	[44]

Notes: active element is Nd^{3+} : YAG (1064 nm); notations are the same as those in Table 1.

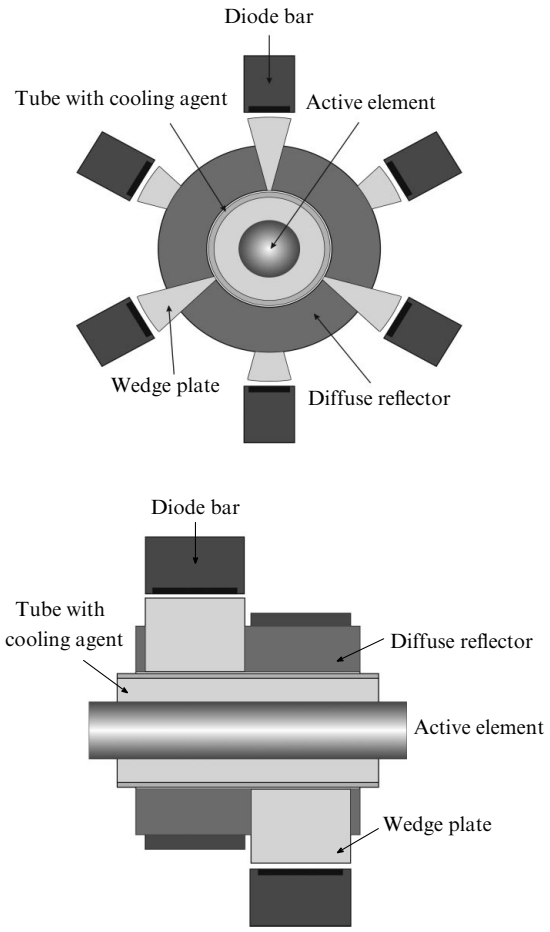

Figure 9. Scheme of a laser head with lens ducts used for coupling pump radiation [45, 46].

such a pump system and a diffuse reflector (see Fig. 9). The coefficient of the radiation transfer by a lens duct achieves 95%. In this case, the total efficiency of the pump power absorption is $\sim 80\,\%$ at good profile uniformity of the absorbed power over the active element volume. Thus, for a $Nd^{3+}:YAG$ laser the efficiencies $\eta_{sl} \leqslant 65\,\%$ and $\eta_{opt} \leqslant 53\,\%$ were obtained [45].

In [47], a scheme is considered for coupling pump radiation from three sources by three glass lens ducts mounted in a single block (transduct). In this pump scheme, the authors obtained a high pump power density of 250 W cm^{-1} (the breakdown threshold for a $Nd^{3+}:YAG$ crystal is about 600 W cm^{-1}) at good uniformity of the inverse population distribution over the active element. Due to a low absorption coefficient in the active element and the absence of the external reflector the laser based on this laser head had poor slope and total efficiencies of 35 % and 29 %, respectively.

Optical systems for radiation input based on cylindrical optical elements capable of increasing the linear pump power density are widely used in laser heads. Cylindrical microlenses (with the diameter of up to 3 mm) are most often used in such systems. They are placed in the vicinity of the pump diode and focus pump radiation onto an active element through input windows on the reflector surface [48 – 53] (see Fig. 10). These systems for radiation input introduce noticeable losses while transmitting radiation. This is caused by several reasons among which the most important are reflection losses, absorption in optical elements, and vignetting of radiation by the reflector input windows. The resulting efficiency of the pump power absorption is 60 % – 80 %. Moreover, the profile of the pump power absorbed in the active element has a well pronounced maximum at the element axis. When such a laser head is used, the slope and total efficiencies for a $Nd^{3+}:YAG$ laser achieve 37 % and 32 %, respectively [49] (see Table 4). In [54, 55], similar variants of the laser head design are considered, however, without an external reflector. The total efficiency of such schemes is lower by 10 % – 15 % than for the schemes with an external reflector.

More complicated schemes for coupling radiation may help obtaining a uniform profile of the absorbed power and

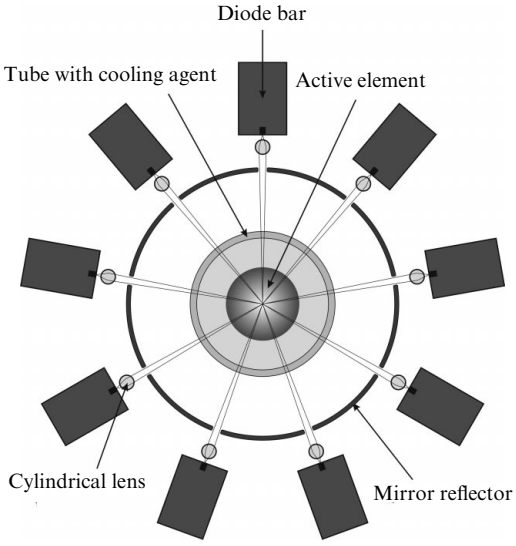

Figure 10. Scheme of a laser head with cylindrical lenses used for coupling pump radiation [48 – 53].

Table 4. Radiation parameters for laser laser heads with cylindrical microlenses used for coupling pump radiation.

d_{ae}/mm	C_a (%)	N_p	η_{sl} (%)	η_{opt} (%)	P_p/W	P_{out}/W	$\frac{P}{L_p}$/W cm^{-1}	M^2	F_{th} (D)	References
4	1.1	9	32.0	29.0	500.0	145.0	55.6	53	7.1	[48]
5	0.9	9	33.3	27.3	1100.0	300.0	61.1	89	6.7	[49]
4	1.1	9	–	31.8	550.0	175.0	61.1	–	4.5	[49]
2	1.0	3	–	23.0	300.0	69.0	–	–	6.7	[50]
2	1.0	3	16.9	12.0	1880.0	225.0	–	–	–	[51]
4	0.6	3	40.8	29.4	9000.0	2650.0	1500.0	–	8.1	[52]
4	–	3	27.7	22.8	850.0	194.0	–	54	13.5	[53]

Notes: active elements are $Yb^{3+}:YAG$ (1030 nm) [50 – 52] and $Nd^{3+}:YAG$ (1064 nm) in the rest references; all the lasers operates in a cw regime; notations are the same as those in Table 1.

the efficiency of the pump power absorption of above 80 %. The cost and complexity of the laser head considerably rise in this case. The scheme for radiation input which comprises a set of cylindrical lenses and trapezoidal lens ducts (see Fig. 11) is presented in [56, 57]. The radiation is coupled into the cavity of a diffuse reflector by means of this optical system. The efficiency of the pump radiation absorption is 82%. This scheme provides very good uniformity of the absorbed energy distribution (see Fig. 12). By using this scheme for pumping a $Nd^{3+}:YAG$ laser, the efficiencies $\eta_{sl} \leqslant 41\,\%$ and $\eta_{opt} \leqslant 32\,\%$ were obtained [57].

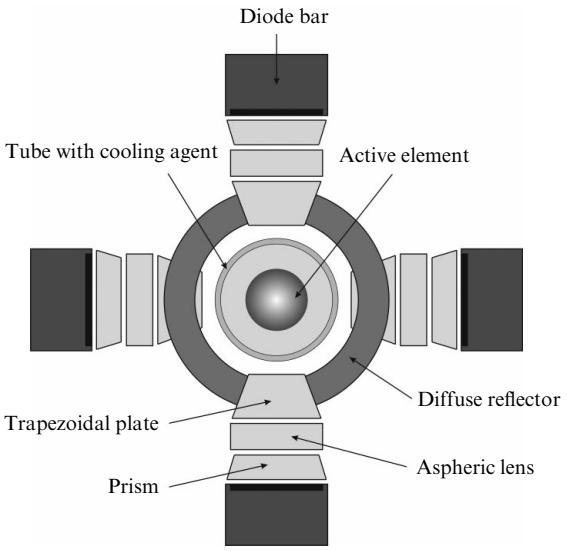

Figure 11. Scheme of the laser head described in [56, 57].

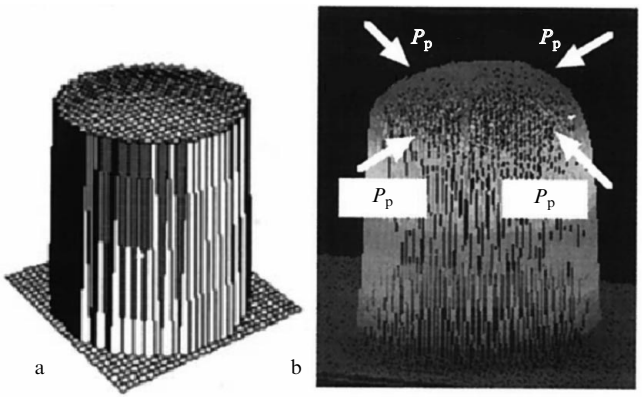

Figure 12. Calculated distribution of the absorbed energy (a) and measured distribution of luminescence (b) across the active element cross section [56, 57].

Fibre systems for coupling radiation have a high efficiency (see Fig. 13) [58]. The pump schemes for with fibre delivery of pump radiatiom are more compact, rational and simple in design. It is not necessary to place pump diodes near the active element in such schemes, which makes the choice of the laser head construction easier, reduces its dimension and mass, and increases the pump power density to 200 – 300 W cm^{-1}. The main drawback is again its high cost and complexity of such systems (first of all, an efficient optical system for coupling radiation into a fibre). A

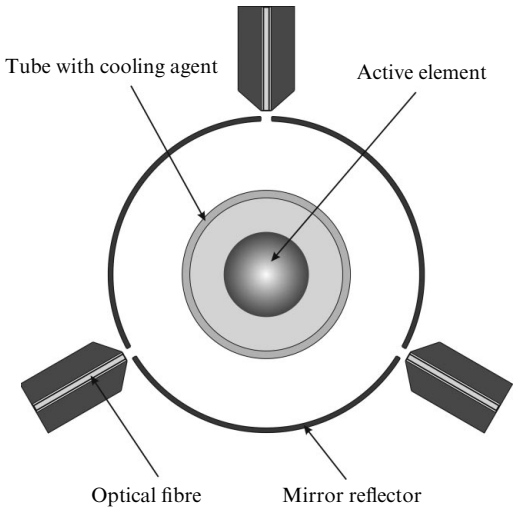

Figure 13. Scheme of a laser head with a fibreoptic system for coupling pump radiation [58].

$Nd^{3+}:YAG$ laser with a fibre system of radiation coupling yields the efficiencies $\eta_{sl} \leqslant 46\,\%$ and $\eta_{opt} \leqslant 43\,\%$ [58].

An original scheme for coupling pump radiation into the active element was proposed in [59] (see Fig. 14). Optical fibres coupling pump radiation are placed tightly against the generatrix of the active element along its optical axis. The fibre cladding in the region of its contact with the surface of the active element is removed. The refractive index of the active element is higher than that of the central part of the fibre; hence, radiation from the fibre is coupled into the active element. The efficiency of the pump radiation absorption in this scheme achieves 90 %. At a greater number of fibres around the generatrix, it is possible to obtain a greater pump power density and good uniformity of the absorbed pump power profile.

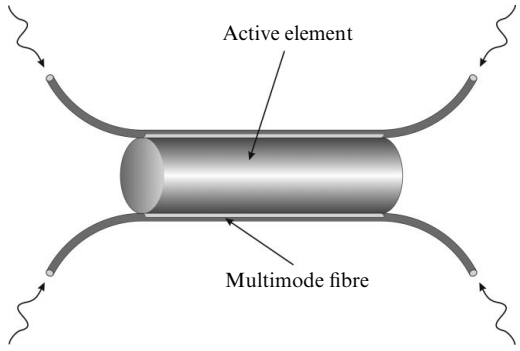

Figure 14. Scheme of fibreoptic pumping [59].

The use of a parabolic concentrator [60] is one more method for coupling pump radiation into the active element. The concentrator consists of two joint parabolic segments, whose foci lie in the opposite segments (see Fig. 15). One end of the concentrator is placed in the cavity of a diffuse reflector, and an assembly of diodes is placed near the other end. The factor of the beam contraction is 13, which gives a greater divergence of pump radiation and provides high uniformity of the absorbed pump radiation profile. The transmission coefficient of such system is $\sim 90\,\%$.

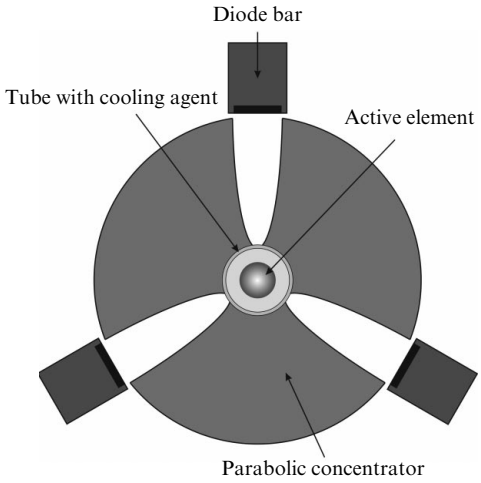

Figure 15. Scheme of a laser head with a parabolic concentrator for coupling pump radiation [60].

The pump scheme used in [61 – 67] is interesting from the practical point of view. In this scheme, pump radiation is focused to the active element by a system of cylindrical lenses and fold mirrors (Fig. 16). The scheme comprises 32 pump channels of this type, placed symmetrically relative to the lateral surface of the active element. Propagation of pump radiation in the cavity of the mirror reflector and multiple transits of pump radiation through the active element provide uniform absorption. By turning the mirrors across the optical axis, pump radiation can be focused into the required region inside the active element. Thus, a possibility arises to vary the absorbed pump power profile in the active element in a wide range. This pump scheme

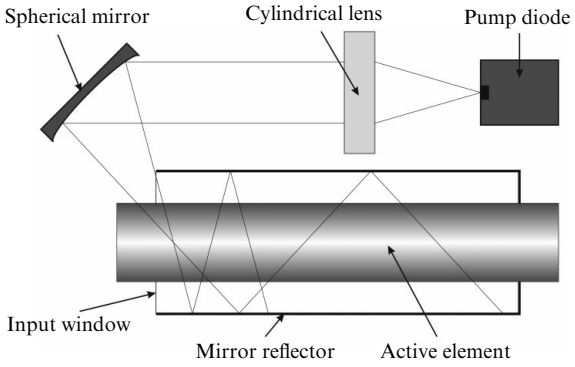

Figure 16. Scheme of the laser head proposed in [61 – 67].

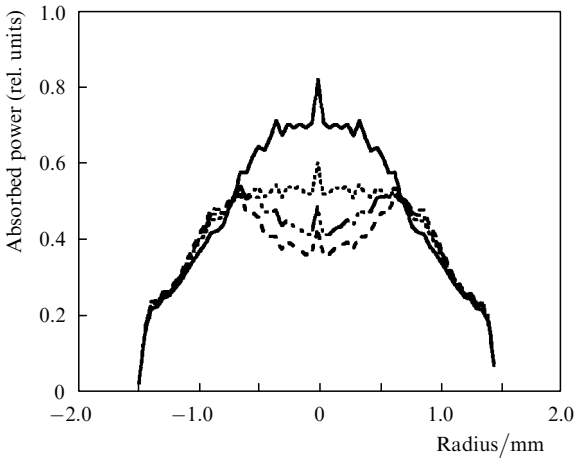

Figure 17. Calculated distributions of the absorbed power at various mirror positions [61 – 67].

makes it possible to form the Gaussian profile of inverse population, which provides efficient generation of TEM_{00}-mode (Table 5). In a single-mode operation regime the slope efficiency of the laser with such a pump system achieves 56 % [61], and the efficiency of the pump power absorption is 90 %. The calculated absorbed energy distributions at various angles of mirrors are shown in Fig. 17.

The scheme for coupling pump radiation with the help of elliptical mirrors, borrowed from flashlamp-pumped systems was considered in [68 – 70]. The elliptical segments are stringently connected with the case of the emitting diode. In one focus of each elliptical segment an active element is placed. In the other focus the output aperture of the diode bar resides (Fig. 18). The coefficient of pump radiation transmission in this scheme is ~ 80 %. The absorbed pump power profile is heavily nonuniform due to the strong focusing of radiation by the elliptical reflectors.

Papers [71 – 75] are interesting from the point of view of research. Authors of these papers consider the efficiency of the pump energy storage (the ratio of the stored energy to the pump energy) for various reflector shapes and materials. The schemes with various reflector shapes for side pumping of the active element are shown in Fig. 19. In these schemes, a cylindrical active element is placed inside a reflector into a solid immerse medium with almost the same refractive index. This provides a more uniform profile of inverse population. The reflecting coating may be diffuse or mirror. Figure 20 presents the dependences of the efficiency of the pump energy storage on the optical density of the medium for the pump schemes with a mirror reflector shown in Fig. 19.

Table 5. Radiation parameters for laser laser heads shown in Fig. 16.

d_{ae}/mm	C_a (%)	η_{sl} (%)	η_{opt} (%)	P_p/W	P_{out}/W	M^2	F_{th}(D)	References
3	0.6	41.2/56.4	31.3/17.0	101.0/166.0	31.6/28.2	–/1.2	4.0	[61]
3	0.6	–/–	33.0/18.6	291.0/199.0	96.0/37.0	–/–	–	[62]
4	0.6	–/46.2	–/14.4	–/291.0	–/42.0	–/–	2.9	[63]
4	0.6	25.0/–	20.0/–	150.0/–	30.0/–	–/–	–	[64]
3	0.6	–/44.8	–/12.8	–/149.0	–/19.0	–/1.1	–	[65]
3	1.0	16.5/–	12.5/–	290.0/–	36.3/–	–/–	7.7	[66]
4	0.6	40.1/–	37.9/–	290.0/–	110.0/–	6/–	–	[67]

Notes: active elements are Nd^{3+} : YAG (1064 nm); all the lasers operates in a cw regime; in the columns separated by "/" left values correspond to multimode operation and right values correspond to single-mode operation; notations are the same as those in Table 1.

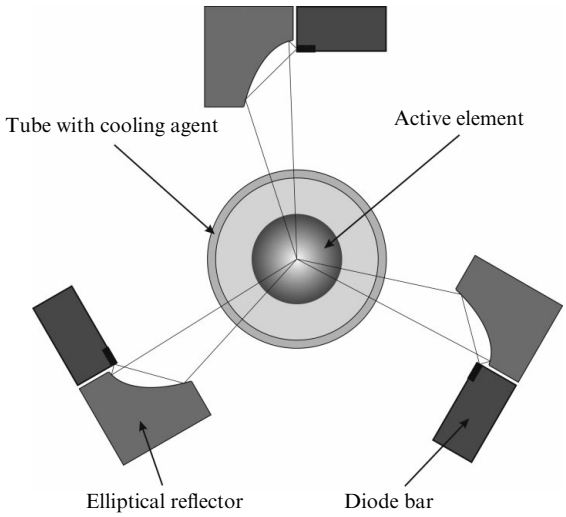

Figure 18. Scheme of a laser head with elliptical mirrors used for coupling pump radiation [68 – 70].

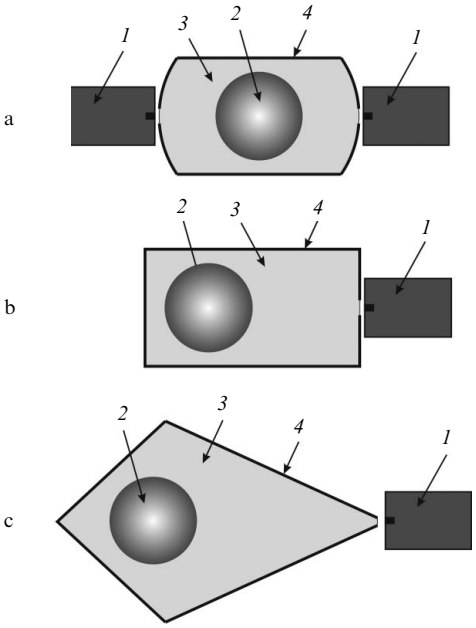

Figure 19. Scheme of side pumping with reflectors of various shapes: (*1*) pump diode, (*2*) active element, (*3*) reflector cavity, (*4*) reflecting coating [71 – 75].

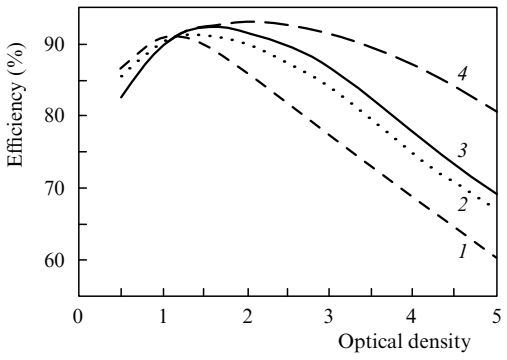

Figure 20. Efficiency of the energy storage versus the optical density for the schemes presented in Fig. 19b (*1*); Fig. 19c (*2*); Fig. 19d (*3*); and for the scheme with a 16-face prism (4).

Moreover, the influence of such parameters as the reflection coefficient, width of input windows, and divergence of pump radiation on the efficiency of the pumping energy storage is analysed in [71 – 75].

There are many alternative ways to obtain a uniform profile of the absorbed pump power over the active element cross section. One of them is delustering of the cylindrical generatrix of the active element [5 – 8, 21, 50 – 52, 56, 57]. Matted active elements compared to polished ones provide a more uniform profile of the absorbed pump power due to the lack of pump radiation focusing by the cylindrical surfaces. In addition, delustering suppresses parasitic field oscillations arising at the boundaries of the active element (whispering gallery modes) and during the reflection from the reflector walls. It is especially important for Q-switched lasers, in which unsuppressed parasitic oscillations considerably reduce the acquired inverse population. However, delustering results in an appearance of surface microcracks on the generatrix, which leads to a noticeable decrease in the thermomechanical breakdown threshold in the active element. The internal surface of the cooling tube can also be matted [6], which enhances the uniformity of the absorbed pump power profile.

The uniform profile of the absorbed pump power can be obtained by changing the diode temperature and thus detuning the wavelength maximum of diode emission from the maximum absorption wavelength of the active element by 2 – 4 nm [5, 39]. The detuning decreases the effective absorption of pump radiation, which provides a more uniform absorption in the active element though reduces the efficiency of the pump radiation absorption. This approach is an alternative to the employment of active elements with a lower activator concentration.

The use of ceramic active elements opens up great possibilities for obtaining a required profile of the absorbed pump power. The production technology provides manufacturing active elements with an arbitrary profile of the activator concentration over their cross section. The employment of the ceramic active element with a doped central part makes it possible to obtain a more uniform profile of the absorbed pump power compared to a similar active element doped uniformly. For example, the active element with the doped central region in the form of hexahedron in the cross section has a smaller gradient of the refraction index over the cross section for other conditions being the same, which is accompanied by approximately a three-fold reduction in the beam quality parameter M^2 [47].

In many cases, a high density of pump power per unit length of the active element is not required and it is sufficient to arrange several (two or three) bars of pump diodes along the generatrix. But obtaining a uniform profile of the absorbed pump power is difficult especially with mirror reflectors. In this case the pump diode bars can be arranged in such a way that each bar is turned by a certain angle around the active element axis [26 – 28, 39 – 44]. In this case, the total profile of the absorbed pump power along the active element length becomes more uniform.

5. Schemes for pumping rectangular elements

Cylindrical active elements have a great drawback, namely, strongly pronounced thermal effects (heat focusing, thermooptical aberrations, thermo-induced birefringence) which

result in a low quality of spatial characteristics for output radiation especially at high output powers. This drawback is mainly related with unfeasibility of efficient cooling of the entire volume of active element because cylindrical elements have the smallest possible lateral area among other elements. An alternative to cylindrical elements are rectangular ('slab') active elements. An intensive investigation of such elements started in the early 80th of the last century. Papers [76–80] present the results of detailed investigations of specific features for radiation propagation and thermal processes in rectangular active elements.

The use of slab elements in lasers noticeably reduces thermal effects. On the one hand, this is achieved due to a greater lateral area of the active element and more uniform cooling of the entire volume. On the other hand, the plane–parallel surfaces favour a waveguide zigzag propagation of generated radiation in the active element, which averages the influence of thermal inhomogeneities on propagating radiation over one coordinate. A rectangular cross section of the active element makes it possible to completely eliminate thermomechanical stresses leading to depolarisation of laser radiation. One more important advantage of slab elements is good overlapping of the pumped region with the domain occupied by generating modes, which determines a higher efficiency of these schemes, especially in a single-mode operation regime.

These advantages are also accompanied by principal drawbacks such as asymmetry and astigmatism of output radiation due to different temperature gradients in orthogonal planes. In addition, the rectangular cross section of the active element determines the rectangular shape of the generated beam, which is inconvenient for many applications. One more drawback is a lower possible pump power density, more difficult fabrication of slab elements, and complicated assembly and adjustment of the laser head construction. At a high gain, amplified spontaneous emission plays a great negative role. Below we consider two laser head types: laser heads with zigzag propagation and with grazing incidence of laser radiation.

5.1 Schemes with zigzag propagation of laser radiation

As was discussed above, one way to reduce the influence of thermal inhomogeneities in an active element is zigzag propagation of generated radiation in the active element volume [80–95]. In such schemes (zigzag schemes), pump radiation is coupled into the active element through one face or through two opposite faces. Optical fibres or cylindrical lenses are often used for radiation coupling; however, the schemes with direct pumping are also employed. In the case of single-sided pumping, a mirror reflector is placed near the opposite face for increasing the efficiency of the pump radiation absorption. In the case of two-sided pumping, radiation should be almost completely absorbed per single pass. In this case, active elements with a high activator concentration or great absorption cross section are used.

Liquid cooling is preferable for slab elements, because it allows one to cool the faces through which optical pumping occurs. In the case of 'dry' conductive cooling, heat is removed from other two faces of the element, through which pump radiation does not pass. The cooling scheme with the use of a diamond plate is also of interest [91]. Pump radiation passes through the diamond plate having an optical contact with a lateral face of the active element. Due to the very high thermal conductivity of diamond this scheme provides efficient cooling of the active element. At the output power of 200 W the optical power of the thermal lens arising in the active element is only 0.04 D.

A zigzag trajectory of the beam is usually arranged in the plane section of the element along which it is pumped and thermal gradients are maximal. In addition, the inverse population in this case is removed more efficiently in the regions where it is maximal. When thin slab elements pumped through the narrow faces and cooled through the wide faces are used, the thermal gradients are maximal between the wide faces [86, 88].

Waveguide propagation of generated radiation between two faces occurs either due to reflections from dichroic mirror surfaces (Fig. 21a) transmitting radiation at the pump wavelength and reflecting radiation at the generation wavelength or due to the total internal reflectance from the faces (Fig. 21b).

In addition to a good compensation of thermal inhomogeneities the zigzag scheme provides sufficiently good overlapping of a generating mode with the pumped volume of active element, which determines a high optical efficiency of the SSL (see Table 6). From this point of view, the schemes with dichroic mirror coatings on faces are most efficient due to a longer optical path of laser radiation and, correspondingly, due to more efficient removal of inverse population [80]. The two-pass schemes with the total internal reflection of the generated beam have a similar advantage (see Fig. 21c) [82, 84, 87].

When dichroic mirror coatings are used on the lateral faces of the active element, parasitic field oscillations arise between these faces, which reduce the inverse population.

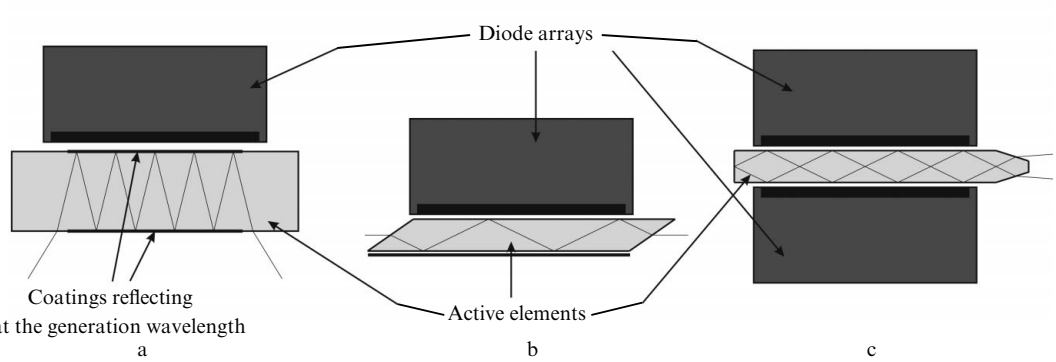

Figure 21. Various realisations of waveguide propagation of generated radiation in the active element [80–95].

Table 6. Radiation parameters for lasers with slab active elements and zigzag ray propagation.

N_p	C_a (%)	η_{sl} (%)	η_{opt} (%)	P_p/W	P_{out}/W	Generation regime	M^2	F_{th} (D)	References
1	1.0	–/46.3	–/30.9	–/9.4	–/2.9	cw	–/1.2	–	[80]
1	1.0	–/43.6	–/33.7	–/9.2	–/3.1	cw	–/1.2	–	[80]
1	–	–/15.9	–/19.0	–/50.4	–/8.0	cw	–/–	–	[81]
1	–	57.0/–	35.0/24.6	18.3	6.4/4.5	cw	–/1.2	–	[82]
2	–	36.0/22.0	30.6/18.9	235.0/212.0	72.0/40.0	cw	–/1.3	1.0	[83]
1	1.1	57.0/–	35.0/25.7	18.3	6.4/4.7	cw	–/1.2	–	[84]
1	–	–/43.8	–/13.5	–/74.0	–/10.0	qcw	–/1.5 × 1.1	1.7 × 0.1	[85]
2	1.0	–/–	42.3/–	300.0/–	127.0/–	cw	–/–	2.4	[86]
2	–	37.0/–	32.0/20.0	100.0	32.0/20.0	cw	–1.4 × 1.2	–	[87]
2	1.0	57.0/22.0	42.3/16.0	300.0/175.0	127.0/28.0	cw	–/1.5	2.4 × 2.1	[88]
2	0.9	–/–	13.9/–	2600.0/–	362.0/–	qcw	–/–	6.7	[90]
1	–	41.0/–	33.3/–	600.0/–	200.0/–	cw	35.0 × 7.0/–	0.04	[91]
2	1.0	18.5/–	12.0/–	1290.0	141.0/–	qcw	180.0 × 16.0/–	–	[92]
2	1.1	34.0/18.2	27.1/12.7	960.0/550.0	260.0/70.0	cw	–/4.0 × 3.0	13.0 × 0.4	[93]
2	–	50.0/50.0	46.2/44.8	78.0/58.0	36.0/26.0	cw	–/1.2 × 1.1	–	[94]
2	–	53.6/46.4	40.5/35.1	37.0	15.0/13.0	cw	–/–	–	[95]

Notes: active elements are Nd^{3+} : YLF (1047 nm) [80, 94], Nd^{3+} : YVO4 (1064 nm) [91,95], and Nd^{3+} : YAG (1064 nm) in the rest references; in the columns separated by "/" left values correspond to multimode operation and right values correspond to single-mode operation; for nonhomocentric beams, the product $M_x^2 \times M_y^2$ is used instead of M^2, and $F_{thx} \times F_{thy}$ is used instead of F_{th}; notations are the same as those in Table 1.

To suppress them, the active element is made slightly wedge-shaped of the order of 0.6 mrad [80].

The zigzag scheme has a great potential in multipass amplifiers due to better employment of the pumped volume of the active element. In this case, the high specific output energy is achieved at a high gain. A multipass amplifier on a slab element was described in [96], which provided the gain $G = 15$ per eight passes at the energy extraction efficiency of 68.1 % (Fig. 22).

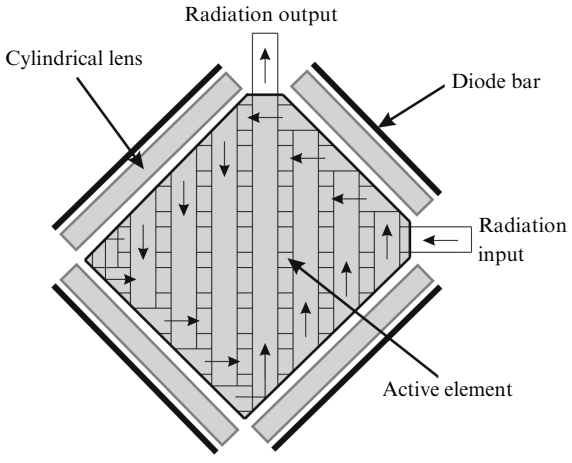

Figure 22. Scheme of the amplifier with a zigzag beam trajectory [96].

The main drawbacks of zigzag schemes are the complexity of producing active elements of required dimensions, complicated cavity adjustment, and high sensitivity to mirror detuning. In addition, in the case of liquid cooling a turbulent flux causes vibrations of the active element, which negatively affects the stability of output radiation.

5.2 Schemes with grazing incidence of laser radiation

A kind of zigzag schemes is the scheme with grazing incidence of laser radiation [97–110]. In this scheme, generated radiation propagates at a small angle (usually 3°–10°) to the face, through which the laser is pumped, and has one total internal reflection on it (Fig. 23a). Pump radiation from a diode bar is focused by cylindrical lenses or lens ducts [105] into a thin 50–100-μm-wide line. Because laser radiation mainly propagates in the boundary (from the pump source side) domain 500 μm thick, highly absorbing active elements with a large absorption cross section (Nd^{3+} : YVO) or a high activator concentration (ceramic Nd^{3+} : YAG) are required. Thus, a small zone with a very high gain is formed in the boundary domain.

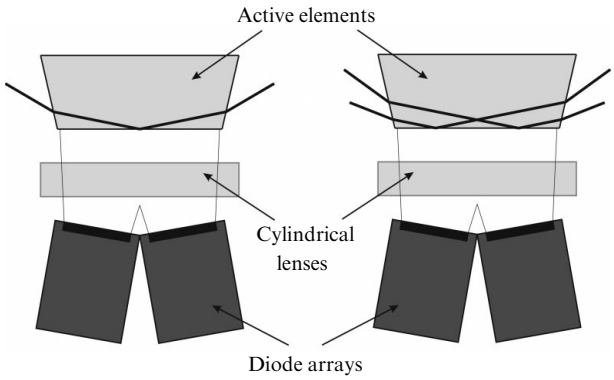

Figure 23. Schemes with grazing incidence of laser radiation [97–110].

Cylindrical lenses are usually placed from both sides of the active element to match the volume of the laser mode with the pumped volume of the active element. This provides a low generation threshold and a high efficiency (see Table 7). A zigzag propagation path of laser radiation averages the influence of thermal effects.

The scheme under study yields the slope and total efficiencies close to a theoretical limit: $\eta_{sl} = 75$ %, $\eta_{opt} = 66$ % for multimode operation and $\eta_{sl} = 68$ %, $\eta_{opt} = 58$ % for single-mode operation [103]. The use of the two-pass scheme (see Fig. 23b) considerably improves the output

Table 7. Radiation parameters for lasers with slab active elements and grazing incidence of radiation.

C_a (%)	η_{sl} (%)	η_{opt} (%)	P_p/W	P_{out}/W	Generation regime	M^2	References
1.1	72.0/69.0	64.3/39.4	35.0	22.5/13.8	qcw	10.0 × 1.0/1.4 × 1.1	[99]
1.1	–/–	35.3/–	17.0	6.0/–	cw	–/–	[100]
1.1	–/58.6	–/53.8	30.5	–/16.4	cw	–/1.3 × 1.2	[101]
1.1	44.0/32.0	38.2/25.3	17.0	6.5/4.3	cw	12.0 × 1.1/1.1	[102]
1.1	–/40.0	–/29.4	17.0	–/5.0	cw	–/1.1	[102]
1.1	74.6/–	65.8/58.5	41.2/39.5	27.1/23.1	cw	10.0 × 1.8/1.3 × 1.1	[103]
1.1	38.0/26.0	33.4/24.4	41.0	13.7/10.0	cw	–/1.1	[104]
1.0	43.0/31.0	40.0/26.6	35.0	14.0/9.3	cw	3.0 × 2.5/1.3	[105]
1.1	62.0/50.2	50.5/45.3	99.7/102.0	50.3/46.2	cw	–/–	[106]
1.1	–/56.2	–/44.1	93.0	–/41.0	cw	–/1.2	[106]
2.0	42.0/–	34.2/–	38.0	13.0/–	cw	12.0 × 1.3/–	[107]
1.1	68.6/46.0	60.4/41.2	83.0/81.0	50.1/34.0	cw	–/1.1	[108]
2.0	31.7/21.8	28.5/17.1	158.0	45.0/27.0	cw	50.0 × 6/1.5	[109]
4.0	14.0/–	10.3/–	11.6	1.2/–	cw	4.1 × 1.6/–	[109]
2.0	49.0/42.0	45.6/38.6	101.0	46.1/39.0	cw	–/1.2	[110]

Notes: active elements are ceramic Nd^{3+}:YAG (1064 nm) [106, 108, 109], Nd^{3+}:GdVO4 (1064 nm) [107], and Nd^{3+}:YVO4 (1064 nm) in the rest references; in the columns separated by "/" left values correspond to multimode operation and right values correspond to single-mode operation; for nonhomocentric beams, the product $M_x^2 \times M_y^2$ is used instead of M^2; notations are the same as those in Table 1.

beam quality and increases the degree of overlapping of the laser mode with the pumped volume [106].

5.3 Schemes with quasi-longitudinal pumping

In high-power SSLs efficient cooling of the active element is required. Due to a small thickness of slab elements a turbulent flux during liquid cooling causes a noticeable vibration of the active element. For this reason, copper heatsinks with microchannel cooling are usually used. To efficiently cool the active element, heat is removed through the faces having greatest area. In high-power systems which require high pump power densities, pumping occurs also through the largest faces. In this case, a scheme with quasi-longitudinal pumping may solve the problem [111 – 116].

In a modification of this scheme the ends of the slab element are skewed at an angle of 45°. Pump radiation passes to them from the side of lateral faces with the help of an optical system. Then after reflection from the ends pump radiation propagates and is absorbed along the optical axis (see Fig. 24). The efficiency of the pump radiation absorption in this scheme is no more than 80%. In this scheme efficient microchannel cooling can be organised through the large faces of the slab element. Generated radiation propagates along a zigzag trajectory inside the active element. With a Nd^{3+}:YAG active element and the pump power of 1400 W this scheme yields the output power of 415 W in the multimode regime and 252 W in the single-mode regime [111].

In another modification of this scheme shown in Fig. 25 the ends of slab element are skewed at the Brewster angle [113 – 116]. The method of pumping is the same; however, the efficiency of the pump radiation absorption in this scheme is ~ 70 %. Generated radiation propagates inside the active element linearly along the optical axis.

One more modification of the schemes considered above is the pump scheme presented in [117 – 120], where an active element is pumped through its skewed faces by means of lens ducts (Fig. 26). Pump radiation propagating inside the active element (with a small activator concentration) due to the total internal reflection is uniformly absorbed in it. In addition, the active element is only activated at its central

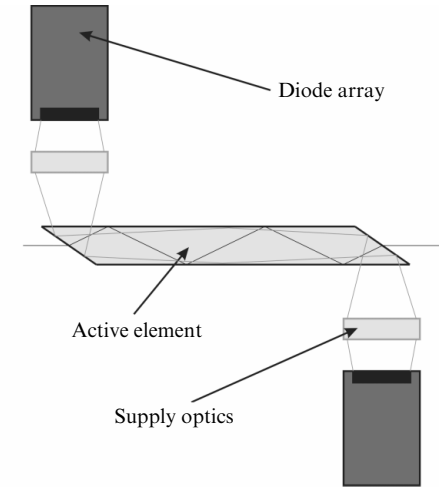

Figure 24. 'Slab' element with quasi-longitudinal pumping [111, 112].

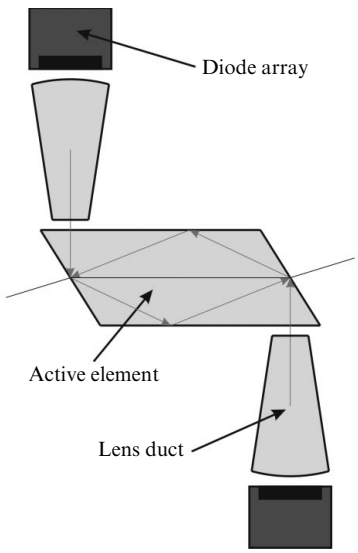

Figure 25. 'Slab' element with quasi-longitudinal pumping [113 – 116].

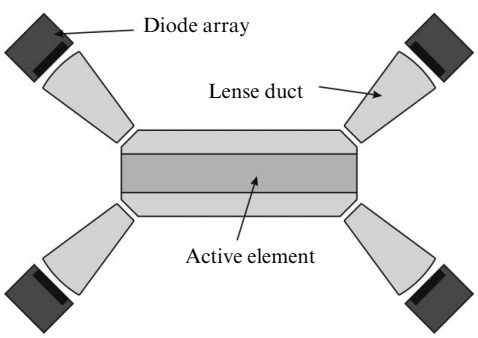

Figure 26. 'Slab' element pumped through skewed ends [117 – 120].

part, which also improves the uniformity of the pump radiation absorption. A zigzag trajectory of generated radiation inside the active element is not required. The efficiency of the pump radiation absorption is ~ 70 %. With a Yb^{+}:YAG active element in this scheme and the pump power of 2000 W, the output power of 520 W was obtained in the multimode regime [118].

5.4 Other schemes for pumping slab elements

In other schemes for pumping slab elements developers use thin active elements with the thickness of several millimeters and linear propagation of generated radiation inside them. In this case the gradients of thermal fields in the active element are sufficiently small and there is no need in a zigzag beam trajectory. The construction of the entire system is noticeably simpler.

Multipass schemes for pumping long slab elements with a small thickness (of the order of a fraction of mm) are widely used. The construction of a laser head with such a pump system is shown in Fig. 27 [121]. The active element is placed in a rectangular cavity of the reflector. Narrow input windows in the reflector cover are used for pumping. The dependence of the efficiency of the pump power absorption on the active element thickness is shown for this scheme in Fig. 28.

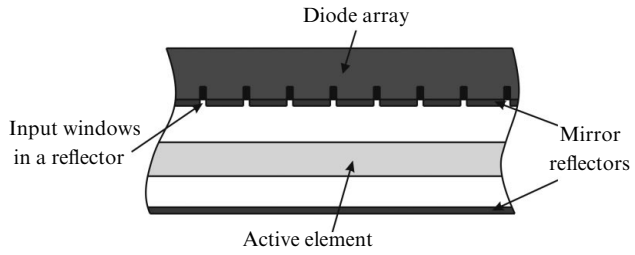

Figure 27. Multipass pumping of a thin 'slab' element [121].

Further evolution of this pump scheme is presented in [122] where instead of the thin active element a planar waveguide with an activated core of thickness 200 μm is used. Waveguide propagation of radiation along this active element compensates for thermal inhomogeneities and more efficiently removes the energy stored in the active element.

Paper [123] is of great research interest where the possibility of using various shapes of mirror condensers is studied for the scheme of pumping a slab element from the viewpoint of the energy storage efficiency and uniformity of

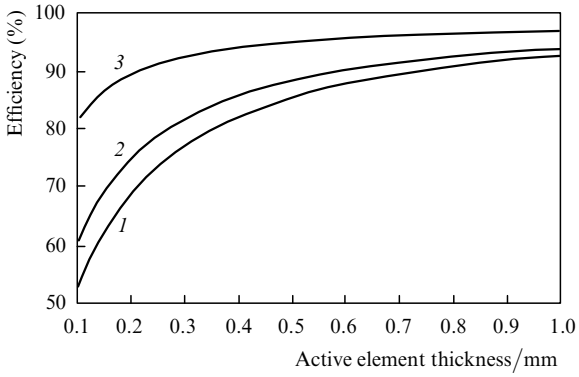

Figure 28. Efficiency of the energy storage versus the thickness of active element with gold coating for the width of input windows 280 μm (*1*) and 100 μm (*2*), and with a dielectric coating for the width of input windows 100 μm (*3*) [121].

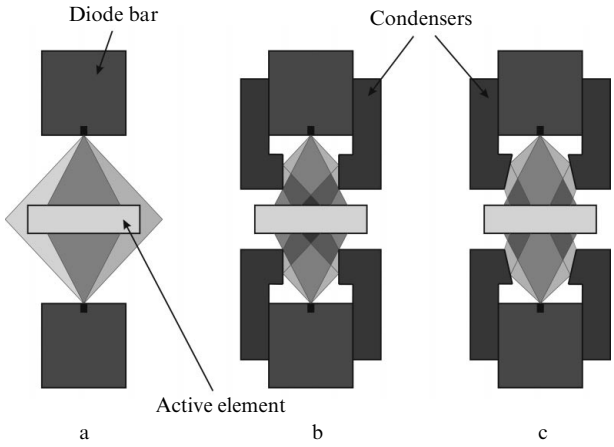

Figure 29. Pumping of 'slab' element without condenser (a), and with mirror plane – parallel (b) and wedge (c) condensers [123].

Table 8. Estimated efficiency of using condensers for pumping 'slab' elements.

Pump scheme	Energy storage efficiency (%)	Degree of profile uniformity for inverse population (%)
Without condenser	70	31
With plane–parallel condenser *	94	53
With wedge condenser **	98	41

* The condenser diameter is 6 mm. ** The condenser diameter is 5 mm, the wedge angle is 10°.

the inverse population profile (Fig. 29). The quantitative estimates found from a numerical simulation are presented in Table 8.

Figure 30 presents laser generation parameters obtained with the pump schemes shown in Fig. 29 for a Nd^{3+}:YAG active element (neodymium concentration is 1%). The most efficient is the pump scheme with a wedge condenser. In this scheme the slope efficiency is ~ 51 %, which is associated with the most efficient energy storage (see Table 8). The most uniform profile is obtained with a plane – parallel condenser.

In some papers a transverse scheme is proposed for pumping a 'quasi-disk' active slab element (see Fig. 31). In this case the thin active element is used, one face of which is

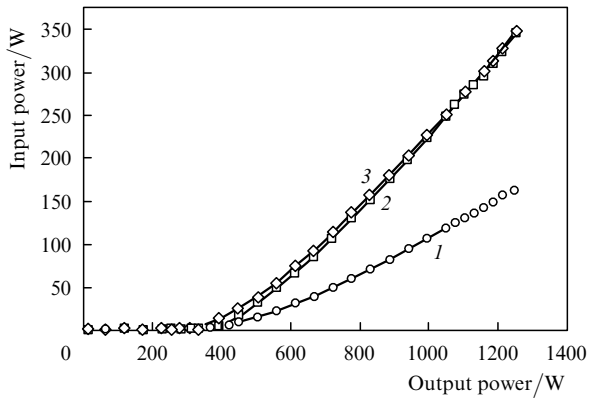

Figure 30. Generation characteristics of a laser obtained with the pump scheme presented in Fig. 29a (*1*), Fig. 29b (*2*), and Fig. 29c (*3*).

in close contact with a copper heatsink. The same face is a highly reflecting mirror of the laser cavity. A highly reflecting coating is deposited on it and then the copper heatsink is soldered to it. In particular, in [124] only the central part of active element is doped with a high activator concentration. In this paper, two $Nd^{3+}:YAG$ active elements were used with the dimensions of $2.0 \times 2.0 \times 0.8$ mm and $1.2 \times 1.2 \times 0.8$ mm and the activator concentrations of 10 % and 15 %, respectively. While using the pump diodes with the fibre-optic output and an optical input radiation system, the efficiency of the energy storage in such samples was 84 % and 79 %, respectively. For increasing this parameter the active element was placed into the cavity of a diffuse reflector.

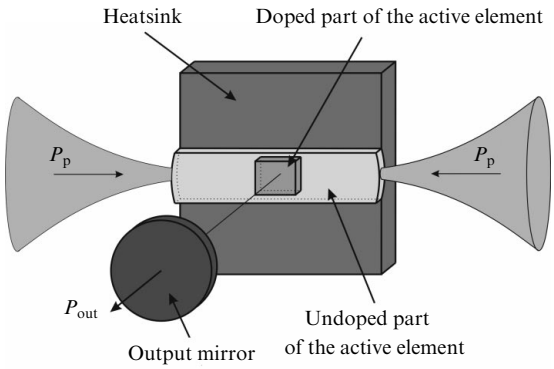

Figure 31. Pumping of a quasi-disk element [124].

Finally, one more pump scheme should be mentioned. A polyhedral active element with a hole at the centre is used in it (Fig. 32) [125]. It is pumped through the lateral faces with the help of forming optics as shown in Fig. 32. The same faces serve as cavity mirrors. A cooling agent passes through the hole and efficiently cools the active element. In addition to a zigzag propagation trajectory for generated radiation this construction substantially reduces the influence of thermal inhomogeneities.

6. Conclusions

Various SSL applications place different requirements to their output characteristics. Hence, there is no universal

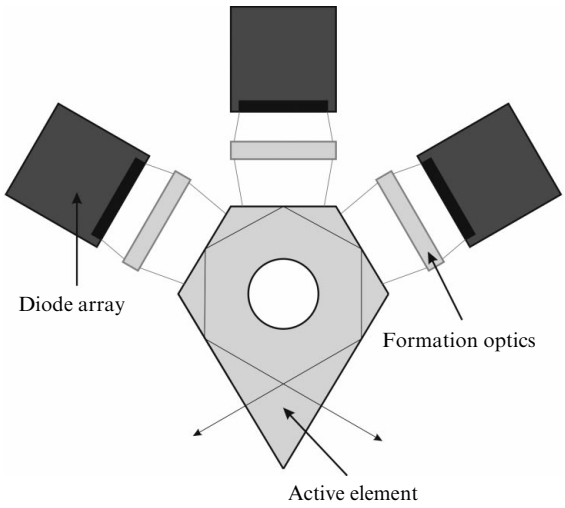

Figure 32. Pumping of a polyhedral active element [125].

scheme for side pumping capable of satisfying all the requirements. An important problem in developing a laser head is the search for an optimal design, which would provide the required characteristics at lowest expenditures.

Almost in all the works the investigation results are presented for laser heads (complete constructions) created with optimal parameters. In developing diode-pumped laser heads the problem of forming a uniform distribution of the pump power over the active element cross section is usually solved. Compared to flashlamp pumping, diode pumping is characterised by a noticeably narrower emission spectrum and a high spatial coherence. This helps forming various types of pump power distributions. Obviously, there exist invariants determining a relation between the element parameters in scaling laser heads with respect to the pump power and the dimension of the active element; however, the functional possibilities of laser heads have not been considered from this point of view. Complex modelling of processes of diode pumping and optimisation of laser head parameters for various purposes require a particular consideration.

Actually there are no papers on laser heads based on active elements with several co-activators and up-conversion active media having several absorption bands. The development of such laser heads requires a combined pump source. Solving of all these problems is awaited.

References

1. Kincade K., Anderson S. *Laser Focus World*, **43**, 82 (2007).
2. Kravtsov N.V. *Kvantovaya Elektron.*, **31**, 661 (2001) [*Quantum Electron.*, **31**, 661 (2001)].
3. Koechner W. *Solid-State Laser Engineering* (Berlin: Springer-Verlag, 1999).
4. Barnes N.P. *IEEE J. Sel. Top. Quantum Electron.*, **13**, 435 (2007).
5. Moon H.-J., Yi J., Han J., Cha B., Lee J. *Appl. Opt.*, **38**, 1772 (1999).
6. Lee S., Yun M., Kim H.S., Cha B.H., Suk S. *Appl. Opt.*, **41**, 1082 (2002).
7. Lee S., Kim S.K., Yun M., Kim H.S., Cha B.H., Moon H.-J. *Appl. Opt.*, **41**, 1089 (2002).
8. Lee S., Yun M., Cha B.H., Kim C.J., Suk S., Kim H.S. *Appl. Opt.*, **41**, 5625 (2002).
9. Wang Y., Kan H. *Opt. Commun.*, **226**, 303 (2003).

10. Sun Z., Li R., Bi Y., Yang X., Bo Y., Zhang Y., Wang G., Zhao W., Zhang H., Hou W. *Opt. Commun.*, **241**, 167 (2004).
11. Yi J., Moon H.-J., Lee J. *Appl. Opt.*, **43**, 3732 (2004).
12. Lee S., Kim Y.G., Cha B.H., Kim Y.K. *Opt. Laser Technol.*, **36**, 265 (2004).
13. Sun Z., Li R., Bi Y., Hu C., Kong Y., Wang G., Zhang H., Xu Z. *Opt. Laser Technol.*, **37**, 163 (2005).
14. Yang X., Bo Y., Peng Q., Zhang H., Geng A., Cui Q., Sun Z., Cui D., Xu Z. *Opt. Commun.*, **266**, 39 (2006).
15. Peng H., Hou W., Chen Y., Cui D., Xu Z., Chen C., Fan F., Zhu Y. *Opt. Express*, **14**, 3961 (2006).
16. Lee S., Choi D., Kim C.-J., Zhou J. *Opt. Laser Technol.*, **39**, 705 (2007).
17. Du K., Zhang J., Quade M., Liao Y., Falter S., Baumann M., Loosen P., Poprawe R. *Appl. Opt.*, **37**, 2361 (1998).
18. Wu R., Phua P.B., Lai K.S. *Appl. Opt.*, **39**, 431 (2000).
19. Wang H., Huang W., Zhou Z., Cao H. *Chin. Opt. Lett.*, **1**, 541 (2003).
20. Wang H., Huang W., Zhou Z., Cao H. *Opt. Laser Technol.*, **36**, 69 (2004).
21. Kandasamy R., Raghavachari S., Misra P., Nathan S. *Appl. Opt.*, **43**, 5855 (2004).
22. Mukhopadhyay P.K. et al. *Opt. Commun.*, **259**, 805 (2006).
23. Haiyong Z., Ge Z., Chenghui H., Yong W., Lingxiong H., Weidong C., Zhenqiang C. *Appl. Opt.*, **46**, 384 (2007).
24. Haiyong Z., Chenghui H., Ge Z., Yong W., Jing C., Weidong C., Zhenqiang C. *Opt. Commun.*, **270**, 296 (2007).
25. Hirano Y., Yanagisawa T., Ueno S., Tajime T., Uchino O., Nagai T., Nagasawa C. *Opt. Lett.*, **25**, 1168 (2000).
26. Ajer H., Landro S., et al. *Opt. Lett.*, **17**, 1785 (1992).
27. Rustad G., Stenersen K. *IEEE J. Sel. Top. Quantum Electron.*, **3**, 82 (1997).
28. Spuhler G.J., Paschotta R., Keller U., Dymott M.J.P., Kopf D., Meyer J., Weingarten K.J. *Opt. Lett.*, **24**, 528 (1999).
29. Brand T. *Opt. Lett.*, **20**, 1776 (1995).
30. Jackson S.D., Piper J.A. *Appl. Opt.*, **33**, 2273 (1994).
31. Jackson S.D., Piper J.A. *Appl. Opt.*, **34**, 2012 (1995).
32. Dawes J.M., Dekker P., Cai Y. *Opt. Commun.*, **115**, 617 (1995).
33. Jackson S.D., Piper J.A. *Appl. Opt.*, **35**, 1409 (1996).
34. Bowman S.R., Lynn J.G., et al. *Opt. Lett.*, **18**, 1724 (1993).
35. Jani M.G., Naranjo F.L., Barnes N.P., et al. *Opt. Lett.*, **20**, 872 (1995).
36. Le Garrec B.J., Raze G.J., et al. *Opt. Lett.*, **21**, 1990 (1996).
37. Qi Y., Zhu X., Lou Q., Ji J., et al. *Opt. Express*, **13**, 8725 (2005).
38. Fujikawa S. et al. *IEEE J. Sel. Top. Quantum Electron.*, **3**, 40 (1997).
39. Kojima T., Yasui K. *Appl. Opt.*, **36**, 4981 (1997).
40. Konno S., Yasui K. *Appl. Opt.*, **37**, 551 (1998).
41. Konno S., Fujikawa S., Yasui K. *Appl. Opt.*, **37**, 6401 (1998).
42. Inoue Y., Fujikawa S. *IEEE J. Quantum Electron.*, **36**, 751 (2000).
43. Konno S., Kojima T., et al. *Opt. Lett.*, **25**, 105 (2000).
44. Konno S., Inoue Y., et al. *Appl. Opt.*, **40**, 4341 (2001).
45. Fujikawa S., Furuta K., Yasui K. *Opt. Lett.*, **26**, 602 (2001).
46. Furuta K., Kojima T., Fujikawa S., Nishimae J. *Appl. Opt.*, **44**, 4119 (2005).
47. Lucianetti A., Weber R., Hodel W., et al. *Appl. Opt.*, **38**, 1777 (1999).
48. Golla D., Knoke S., Schone W., Tunnermann A., Schmidt H. *Appl. Phys. B*, **58**, 389 (1994).
49. Golla D., Knoke S., Schone W., et al. *Opt. Lett.*, **20**, 1148 (1995).
50. Bruesselbach H.W., Sumida D.S. *Opt. Lett.*, **21**, 480 (1996).
51. Bruesselbach H.W., Sumida D.S., Reeder R.A., Byren R.W. *IEEE J. Sel. Top. Quantum Electron.*, **3**, 105 (1997).
52. Bruesselbach H.W., Sumida D.S. *IEEE J. Sel. Top. Quantum Electron.*, **11**, 600 (2005).
53. Roth M.S., Romano V., Feurer T., Graf T. *Opt. Express*, **14**, 2191 (2006).
54. Golla D., Freitag I., Zeilmer H., Schone W., Kropke I., Welling H. *Opt. Commun.*, **98**, 86 (1993).
55. Yu D.L., Tang D.Y. *Opt. Laser Technol.*, **35**, 37 (2003).
56. Hirano Y., Koyata Y., et al. *Opt. Lett.*, **24**, 679 (1999).
57. Pavel N., Hirano Y., Yamamoto S., Koyata Y., Tajime T. *Appl. Opt.*, **39**, 986 (2000).
58. Howerton P.H., Cordray D.M. *IEEE J. Sel. Top. Quantum Electron.*, **28**, 1081 (1992).
59. Golla D., Bode M., Knoke S., Schone W., Tuennermann A. *Opt. Lett.*, **21**, 210 (1996).
60. Lai K.S., Phua P.B., Wu R.F., et al. *Opt. Lett.*, **25**, 1591 (2000).
61. Uehara N., Nakahara K., Ueda K. *Opt. Lett.*, **20**, 1707 (1995).
62. Song J., Liu A., Okino K., Ueda K. *Appl. Opt.*, **36**, 8051 (1997).
63. Song J., Liu A.P., Shen D.Y., Ueda K. *Appl. Phys. B*, **66**, 539 (1998).
64. Song J., Shen D., Liu A., et al. *Appl. Opt.*, **38**, 5158 (1999).
65. Song J., Li C., Kim N.S., Ueda K. *Appl. Opt.*, **39**, 4954 (2000).
66. Lu Jun., Lu Jian., Murai T., Takaichi K., Uematsu T., Xu J., Ueda K., Yagi H., Yanagitani T. *Opt. Lett.*, **27**, 1120 (2002).
67. Lu J., Yagi H., Takaichi K., et al. *Appl. Phys. B*, **79**, 25 (2004).
68. Greiner U.J., Klingenberg H.H., Walker D.R., Flood C.J., van Driel H.M. *Appl. Phys. B*, **58**, 393 (1994).
69. Walker D.R., Flood C.J., van Driel H.M., Greiner U.J., Klingenberg H.H. *Opt. Lett.*, **19**, 1055 (1994).
70. Greiner U.J., Klingenberg H.H. *Opt. Lett.*, **19**, 1207 (1994).
71. Yang H. *Opt. Commun.*, **204**, 263 (2002).
72. Geng A., Bo Y., Bi Y., Sun Z., Yang X., Peng Q., Li H., Li R., Cui D., Xu Z. *Opt. Lasers Eng.*, **44**, 589 (2006).
73. Boutchenkov V., Kuchma I., Levoshkin A., Mak A., Petrov A., Hollemann G. *Opt. Commun.*, **177**, 383 (2000).
74. Levoshkin A., Petrov A., Montagne J.E. *Opt. Commun.*, **185**, 399 (2000).
75. Mak A.A., Soms L.N., Fromzel V.A., Yashin V.E. *Lazery na stekle s neodimom* (Neodymium Glass Lasers) (Moscow: Nauka, 1990).
76. Mezenov A.V., Soms L.N., Stepanov A.I. *Termooptika tverdotel'nykh lazerov* (Thermooptics of Solid-State Lasers) (Leningrad: Mashinostroenie, 1986).
77. Kane T.J., Eckardt R.C., Byer R.L. *IEEE J. Quantum Electron.*, **19**, 1351 (1983).
78. Eggleston J.M., Kane T.J., Kunh K., Unternahrer J., Byer R.L. *IEEE J. Quantum Electron.*, **20**, 289 (1984).
79. Kane T.J., Eggleston J.M., Byer R.L. *IEEE J. Quantum Electron.*, **21**, 1195 (1985).
80. Baer T.M., Head D.F., Gooding P., Kintz G.J., Hutchison S. *IEEE J. Quantum Electron.*, **28**, 1131 (1992).
81. Farinas A.D., Gustafson E.K., Byer R.L. *Opt. Lett.*, **19**, 114 (1994).
82. Richards J., McInnes A. *Opt. Lett.*, **20**, 371 (1995).
83. Shine R.J. Jr, Alfrey A.J., Byer R.L. *Opt. Lett.*, **20**, 459 (1995).
84. McInnes A., Richards J. *IEEE J. Quantum Electron.*, **32**, 1243 (1996).
85. Armandillo E., Norrie C., Cosentino A., Laporta P., Wazen P., Maine P. *Opt. Lett.*, **22**, 1168 (1997).
86. Rutherford T.S., Tulloch W.M., Gustafson E.K., Byer R.L. *IEEE J. Quantum Electron.*, **36**, 205 (2000).
87. Mudge D., Ostermeyer M., Veitch P.J., Munch J., Ottaway D.J., Hamilton M.W. *IEEE J. Sel. Top. Quantum Electron.*, **6**, 643 (2000).
88. Rutherford T.S., Tulloch W.M., Sinha S., Byer R.L. *Opt. Lett.*, **26**, 986 (2001).
89. Kiriyama H., Yamakawa K., Nagai T. *Opt. Lett.*, **28**, 1671 (2003).
90. Malinin B.G., Mak A.A., Volynkin V.M., Gratsianov K.V., Eremenko A.S., Mit'kin V.M., Pankov V.G., Serebryakov V.A., Ustyugov V.I., Chizhov S.A., Yashin V.E. *J. Opt. Technol.*, **70**, 905 (2003).
91. Tzuk Y., Tal A., Goldring S., Glick Y., Lebiush E., Kaufman G., Lavi R. *IEEE J. Quantum Electron.*, **40**, 262 (2004).
92. Ciofini M., Lapucci A. *Appl. Opt.*, **43**, 6174 (2004).
93. Ranganathan K., Misra P., Nath A.K. *Appl. Phys. B*, **86**, 215 (2007).
94. http://www.qpeak.com/Products/MPS.cwlasers.htm.
95. http://www.qpeak.com/Products/MPV.cwlasers.htm.
96. Coyle D.B. *IEEE J. Quantum Electron.*, **27**, 2327 (1991).
97. Bernard J.E., Alcock A.J. *Opt. Lett.*, **18**, 968 (1993).
98. Bernard J.E., Alcock A.J. *Opt. Lett.*, **19**, 1861 (1994).

99. Damzen M.J., Trew M., Rosas E., Crofts G.J. *Opt. Commun.*, **196**, 237 (2001).
100. Garcia-Lopez J.H., Aboites V., Kir'yanov A.V., Holmgren S., Damzen M.J. *Opt. Commun.*, **201**, 425 (2002).
101. Garcia-Lopez J.H., Aboites V., Kir'yanov A.V., Damzen M.J., Minassian A. *Opt. Commun.*, **218**, 155 (2003).
102. Bermudez-Gutierrez J.C., Damzen M.J., Pinto-Robledo V.J., Kir'yanov A.V. *Appl. Phys. B*, **76**, 12 (2003).
103. Minassian A., Thompson B., Damzen M.J. *Appl. Phys. B*, **76**, 341 (2003).
104. Minassian A., Damzen M.J. *Opt. Commun.*, **230**, 191 (2004).
105. Zimer H., Albers K., Wittrock U. *Opt. Lett.*, **29**, 2761 (2004).
106. Minassian A., Thompson B., Damzen M.J. *Opt. Commun.*, **245**, 295 (2005).
107. Omatsu T., Isogami T., Minassian A., Damzen M.J. *Opt. Commun.*, **249**, 531 (2005).
108. Minassian A., Thompson B.A., Smith G., Damzen M.J. *IEEE J. Sel. Top. Quantum Electron.*, **11**, 621 (2005).
109. Omatsu T., Ojima Y., Minassian A., Damzen M.J. *Opt. Express*, **13**, 7011 (2005).
110. Sauder D., Minassian A., Damzen M.J. *Opt. Express*, **14**, 1079 (2006).
111. Goodno G.D., Palese S., Harkenrider J., Injeyan H. *Opt. Lett.*, **26**, 1672 (2001).
112. Goodno G.D., Weiss S.B., Redmond S., Simpson R., Howland D., Weber M., Injeyan H. *Opt. Lett.*, **31**, 1247 (2006).
113. Sudesh V., Asai K., Shimamura K., Fukuda T. *Opt. Lett.*, **26**, 1675 (2001).
114. Sudesh V., Asai K., Shimamura K., Fukuda T. *IEEE J. Quantum Electron.*, **38**, 1102 (2002).
115. Sudesh V., Asai K. *J. Opt. Soc. Am. B*, **20**, 1829 (2003).
116. Sato A., Asai K., Mizutani K. *Opt. Lett.*, **29**, 836 (2004).
117. Gong M., Li C., Liu Q., Chen G., Gong W., Yan P. *Appl. Phys. B*, **79**, 265 (2004).
118. Liu Q., Gong M., Lu F., Gong W., Li C. *Opt. Lett.*, **30**, 726 (2005).
119. Gong M., Lu F., Liu Q., Gong W., Li C. *Appl. Opt.*, **45**, 3806 (2006).
120. Lu F., Gong M., Xue H., Liu Q., Gong W. *Opt. Laser Technol.*, **39**, 949 (2007).
121. Faulstich A., Baker H.J., Hall D.R. *Opt. Lett.*, **21**, 594 (1996).
122. Lee J.R., Baker H.J., Friel G.J., Hilton G.J., Hall D.R. *Opt. Lett.*, **27**, 524 (2002).
123. Lapucci A., Ciofini M. *Appl. Opt.*, **44**, 4388 (2005).
124. Dascalu T., Taira T., Pavel N. *Opt. Lett.*, **27**, 1791 (2002).
125. Ziolek C., Ernst H., Will G.F., Lubatschowski H., Welling H., Ertmer W. *Opt. Lett.*, **26**, 599 (2001).